A Fast and Efficient Codebook-Based RIS Phase Configuration Method

Abdullah Haskou, Hamidreza Khaleghi

A Fast and Efficient Codebook-Based RIS Phase Configuration Method

Abdullah Haskou, Hamidreza Khaleghi
b<>com
1219 Avenue des Champs Blancs, 35510 Cesson-Sévigné, France
Email: {abdullah.haskou, hamidreza.khaleghi}@b-com.com

***Abstract*—Reconfigurable Intelligent Surfaces (RISs) consist of large array of low-cost passive elements that can be configured in real-time to alter the wavefront of incident electromagnetic waves and enhance communication system performances. However, as the number of RIS elements increases the RIS phase configuration overhead also increases. To reduce this overhead, a codebook-based approach can be used where the RIS is preset with a limited number of configurations. However, the selection of the quasi-optimal configuration, from the set of available predefined configurations, still presents a relatively high overhead. In this paper, we propose a multi-level multi-width beam sweeping method for fast, efficient and low-overhead RIS configuration.**

Keywords—Reconfigurable Intelligent Surface (RIS), codebook-based beamforming, configuration overhead

I. INTRODUCTION

A Reconfigurable Intelligent Surface (RIS) is a programmable structure that can be used to control electromagnetic (EM) waves' propagation [1]. Indeed, a RIS is a planar surface made up of an array of passive reflecting elements, each of which can independently alter the phase of the incoming signal. By properly adjusting the phase shifts, the reflected signals can be redirected to the desired direction [2-5]. There are different types of RISs, including reflecting, refracting, focusing, absorbing surfaces and more. They can be passive or active, with or without amplification. Applications of RISs include coverage enhancement, localization and sensing, energy saving, and more. In [6], an overview of RIS enabled opportunities for 5G-Advanced is provided and some critical requirements and challenges are highlighted from a standardization perspective. The latest progress in research, development and standardization on RISs is presented in [7]. Several works have studied practical implementations of discrete-phase RIS. In [8], the authors reported early field trial results of RISs in 5G networks. The experimental results showed that RISs can solve coverage issues and improve received signal quality in 5G networks across different frequency bands.

Despite the potential benefits of RISs, there are still several challenges that need to be addressed before they can be widely adopted. One of the main challenges is the accurate and continual estimation of the cascaded-channel between the transmitting and receiving points through the RIS, which can have a very important overhead on the network [9]. To address this, a codebook-based approach has been proposed [10], where the number of possible RIS configurations is limited to a set of preconfigured beams. However, this still requires channel estimation for all the preconfigured beams and is not energy-efficient. In this paper we propose a fast and efficient beam selection method using a codebook. The method significantly reduces the number of beams tested, yet maintains the same level of performances as if all the preset beams were tested.

II. SYSTEM MODEL

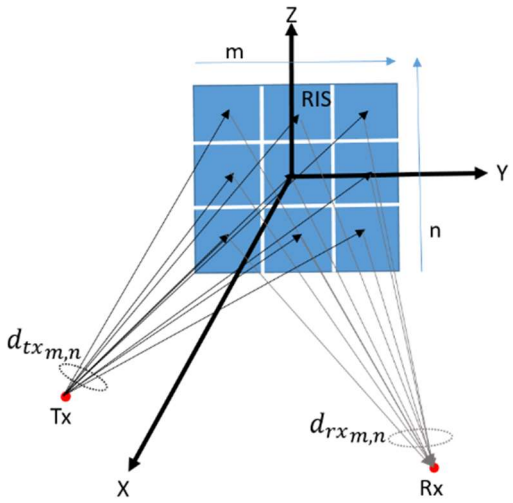

Figure 1. An example of a RIS-aided communication system.

We consider a RIS-aided communication system consisting of a transmitter (Tx), a receiver (Rx), and a RIS made up of multiple RIS elements (m, n) as depicted in Figure 1 (which is just a schematic representation and not to scale). The complex reflection coefficient of each RIS element (m, n) is denoted as:

$$\Gamma_{m,n} = |\Gamma_{m,n}| e^{j\varphi_{m,n}} \tag{1}$$

where $|\Gamma_{m,n}|$ is the reflection magnitude and $\varphi_{m,n}$ is the reflection phase of the element.
Assuming the reflection magnitude of all the RIS elements is equal to one (i.e., $|\Gamma_{m,n}| = 1$), the complex reflection coefficient can be simplified to:

$$\Gamma_{m,n} = e^{j\varphi_{m,n}} \tag{2}$$

We assume that the RIS is located in the far-field region of both the transmitter and the receiver, and there is only a Line-of-Sight (LoS) path from- and to- the RIS. The far-field region's inner radius for an antenna with the largest dimension D is calculated as $R = \frac{2D^2}{\lambda}$ [11]. Therefore, the received signal can be calculated using a free-space propagation model with far-field approximations (ignoring the additive noise) as:

$$s_{rx} = \frac{s_{tx}\lambda^2\sqrt{G}}{(4\pi)^2 d_{tx} d_{rx}} \sum_{m=1}^{M}\sum_{n=1}^{N} e^{j\left(\varphi_{m,n} - k\left(d_{tx_{m,n}} + d_{rx_{m,n}}\right)\right)} \tag{3}$$

where s_{tx} is the trasmitted complex signal, λ is the free-space wavelength, $k = \frac{2\pi}{\lambda}$ stands for the wave number, d_{tx}, d_{rx} are respectively the distance from the RIS central element to Tx and Rx, and $d_{tx_{m,n}}$, $d_{rx_{m,n}}$ are the distance from the (m,n) element respectively to Tx and Rx, and G represents the overall gain between Tx and Rx through RIS.

To maximize the received signal's amplitude, all signals reflected by RIS elements must arrive in phase at the receiver. Hence:

$$\varphi_{m,n} - k\left(d_{tx_{m,n}} + d_{rx_{m,n}}\right) = \varphi_0 \tag{4}$$

$$\rightarrow \varphi_{m,n} = \varphi_0 + k\left(d_{tx_{m,n}} + d_{rx_{m,n}}\right) \tag{5}$$

Setting $\varphi_0 = 0$, the required phase is given by [3]:

$$\varphi_{m,n} = k\left(d_{tx_{m,n}} + d_{rx_{m,n}}\right) \tag{6}$$

The last equation demonstrates that the calculated RIS phases makes the RIS reciprocal, meaning that the same RIS phases can be utilized for both uplink and downlink transmissions. By incorporating (6) into (3), we obtain a received signal that can be expressed as:

$$s_{rx} = \frac{s_{tx} NM\sqrt{G}\lambda^2}{(4\pi)^2 d_{tx} d_{rx}} \tag{7}$$

Therefore, the amplitude of received signal increases propotionally with the number of RIS elements $(N \times M)$, indicating that the received signal power and SNR increase quadratically with the number of the elements [4].

III. Proposed Solution

Figure 2(a) depicts a schematic illustration of the proposed RIS beam selection method using two beam levels. In beam sweeping procedure, the RIS is preconfigured with *M* narrow beams, shown as filled lines in the figure. We propose instead to preconfigure the RIS with *K* wide beams, depicted as dotted lines. A wide beam can be viewed as an aggregation of *N* narrow beams. The RIS first tests the *K* wide beams and selects the one that provides the best performance (SNR, capacity, etc.) for the user equipment. Then, it tests the *N* narrow beams within the selected wide beam to choose the one that delivers the best performance. This approach reduces the number of tested beams from M to $L = K + N$ while maintaining the same performance. For instance, in the illustrated example, we set $M = 21$, $N = 7$ and $K = 3$, which results in a reducing the number of tested beams from 21 to 10. Additionally, to further minimize the number of tested beams, intermediate beam levels can be introduced as shown in Figure 2(b).

A. Optimal number of wide beams in two-level beams case

Here, our aim is to compute the optimal number of wide beams. This can be done by calculating the derivative of the required number of tested beams *L* with respect to the number narrow beams *N*, and equating it to zero, as illustrated below:

$$L = K + N = \frac{M}{N} + N \tag{8}$$

$$\frac{\partial L}{\partial N} = \frac{-M}{N^2} + 1 = 0 \tag{9}$$

$$N = \sqrt{M} \rightarrow K = \sqrt{M} \rightarrow L = 2\sqrt{M} \tag{10}$$

We formulate the reduction factor δ for the number of tested beams as follows:

$$\delta = \frac{M - 2\sqrt{M}}{M} = 1 - \frac{2}{\sqrt{M}} \tag{11}$$

This implies that, as the number of narrow beams increases, the reduction factor also increases. Figure 3 depicts the number of tested beams when there are 100 narrow beams, as a function of the number of regrouped beams. As seen, in the single-level scenario, the minimum number of tested configurations occurs at $N = 10$, which is in accordance with the calculated optimal solution given in (10). Figure 4 shows the reduction factor for the number of tested beams, calculated using the proposed optimal solution, as a function of the number of narrow beams. This demonstrates the advantage of this approach for a large number of narrow beams.

B. Optimal number of levels in multi-level beams case

Now, considering that *N* beams are grouped together from one beam level to the next higher level. This results in a logarithmic tree with a base of *N*, and the number of the beam levels is given by:

$$I = log_N(M) \tag{12}$$

Therefore, the total number of configurations that need to be tested when *N* beams are grouped together at each level is given by:

$$L = N.I = N.log_N(M) = N.\frac{\ln(M)}{\ln(N)} \tag{13}$$

The optimal number of wide beams for this case can be calculated as follows:

$$\frac{\partial L}{\partial N} = 0 \rightarrow N = e \rightarrow I = \ln(M) \rightarrow L = e.ln(M) \tag{14}$$

As depicted in Figure 3, this setup reaches the optimal solution for $N = e$. Since the number of regrouped beams must be an integer, $N = 2$ or $N = 3$ can be selected. In this case, the reduction factor for the number of tested beams can be computed as follows:

$$\delta = \frac{M - N\log_N M}{M} = 1 - \frac{N\log_N(M)}{M} \tag{15}$$

This implies that, similarly to the previous two-level scenario, the reduction factor grows with the increase in the number of narrow beams. Figure 4 shows the reduction factor for $N =$

3, and it is apparent that this multi-level solution outperforms the previous mentioned two-level solution.

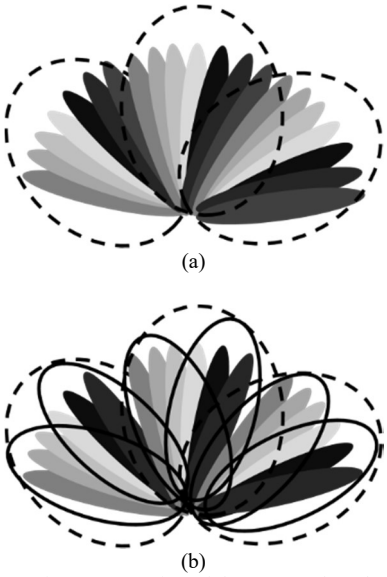

Figure 2. A schematic representation of the proposed method. (a) With two level beams (b) with multi-level beams.

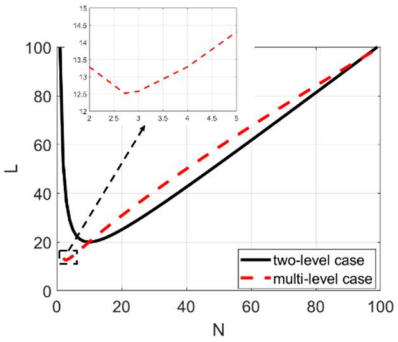

Figure 3. Derivation of the optimal number of regrouped beams for M=100.

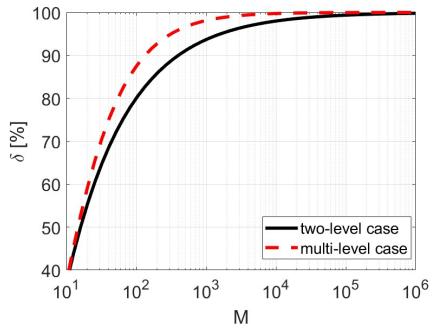

Figure 4. Number of tested beams reduction factor using the proposed optimal solutions.

IV. Practical Realization

A. Narrow beam realization

Let us consider a RIS in the YoZ plane and a transmitter and receiver in the XoY plane as shown in Figure 1. This RIS, of a 21×21 elements, is designed for 3.75 GHz 5G's band with an inter-element distance of half a wavelength. Using spherical coordinate system $(r, \theta, \emptyset)$, the RIS is centered at $(0m, 0°, 0°)$ and the Tx is located at $(40m, 90°, -10°)$. Four cases are considered, where the Rx is located at respectively $(160m, 90°, -30°)$, $(120m, 90°, 0°)$, $(100m, 90°, 30°)$ and $(140m, 90°, 60°)$. The different cases were simulated using MATLAB. Figure 5 shows the calculated required magnitude of every RIS element in the four cases. Figure 6 illustrates the required phase calculated for every RIS element in the four cases. Figure 7 (the inset) shows the relative received power (normalized to have a maximum value of 0 dB) in the horizontal plane (XoY plane). As it can be seen, in all the four cases (corresponding to the four different Rx locations), the received power is maximized in Rx direction (a beam is successfully formed in Rx direction). The obtained beamwidth can be calculated by taking the power level on a circle centered at the RIS center and passing by Rx location. The obtained patterns in this scenario are given by the blue-dashed curves in Figure 7. The Half Power Beamwidth (HPBW) (i.e., the angle at which the power reduces by 3dB from its maximum value, on both sides of the maximum value) in the horizontal plane in the four cases is respectively around 5.6°, 4.8°, 5.6° and 9.8°. This means that, as expected, the best beam formation is achieved in the RIS axis (i.e., for $\emptyset = 0°$). The HPBW in the vertical plane for all cases is around 4.8° (the figure is not shown).

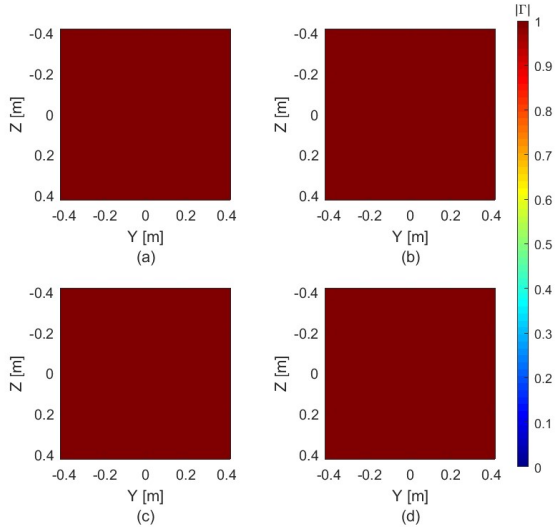

Figure 5. Required RIS reflection coefficient magnitudes in the 4 different cases. (a) Case 1, (b) case 2, (c) case 3 and (d) case 4.

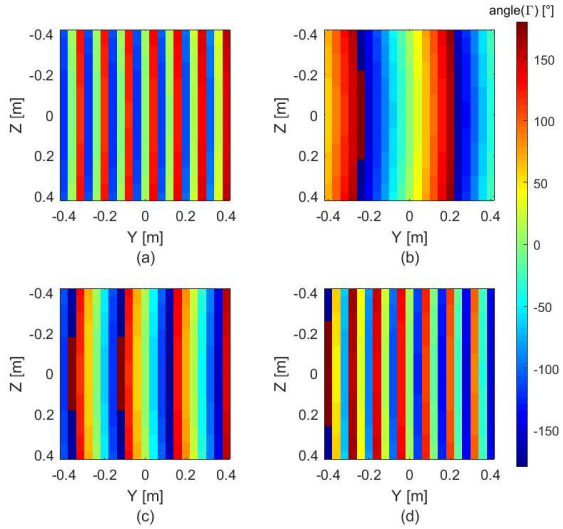

Figure 6. Required RIS phases in the 4 different cases. (a) Case 1, (b) case 2, (c) case 3 and (d) case 4.

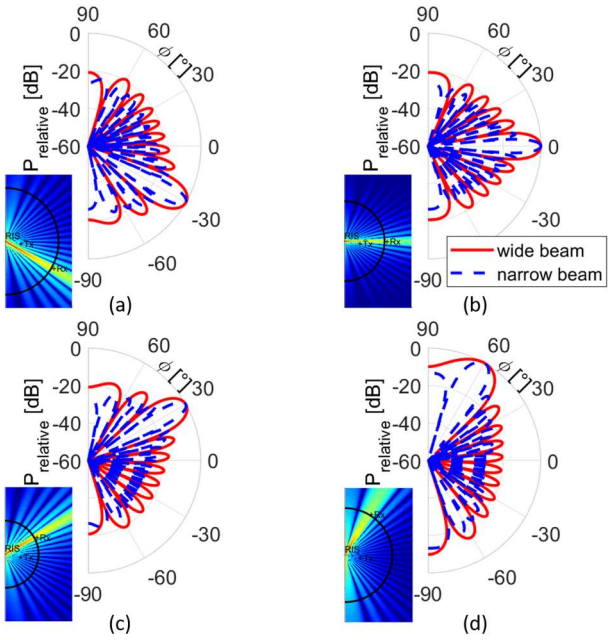

Figure 7. Beamwidth calculation method (in the inset) and obtained beams in the horizontal plane in the 4 different cases. (a) Case 1, (b) case 2, (c) case 3 and (d) case 4.

B. Wide beam realization

The RISs' beamwidth can be easily widened by setting the complex reflection coefficient of some elements to zero (switching off some elements). Taking the previous example and using 11×11 central elements while setting the reflection coefficient of the others to zero, as shown in Figure 8 and Figure 9, the resulted beam can be widened. The obtained patterns in the horizontal plane in this scenario are given by the red curves in Figure 7. The HPBW in the horizontal plane in the four cases is respectively around 10.7°, 9.2°, 10.7° and 19.4°. The HPBW in the vertical plane for the four cases is around 9.2° (the figure is not shown). It should be noted, that the RISs' beamwidth in the two planes can be controlled independently by controlling the number of active RIS elements in that plane. Indeed, reducing the number of active RIS elements in Y-direction will only affect the beamwidth in XoY plane. Similarly, reducing the number of active RIS elements in Z-direction will only affect the beamwidth in the vertical plane. In the taken example, only reducing the number of active RIS elements in Y-direction to 11, while leaving the number of active elements in Z-direction at 21, the obtained HPBW in the XoY plane are still 10.7°, 9.2°, 10.7° and 19.4°, but the vertical HPBW are unchanged compared to the original case (around 4.8°). Furthermore, it can be shown by simulations that multiplying the number of active elements by a factor α, divides the HPBW by approximately the same factor.

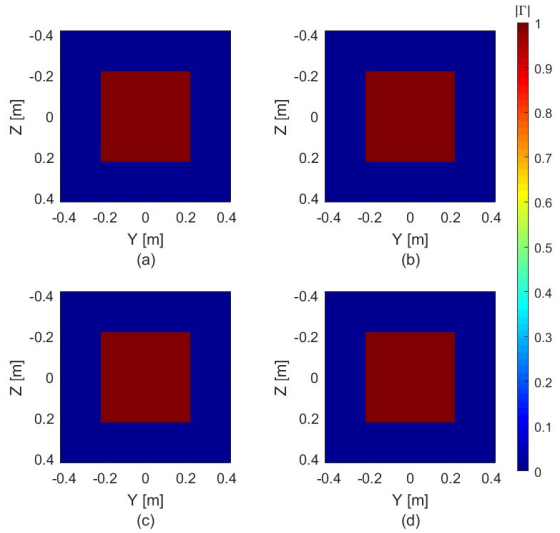

Figure 8. Required RIS reflection coefficient magnitudes in the 4 different cases for a wider beamwidth. (a) Case 1, (b) case 2, (c) case 3 and (d) case 4.

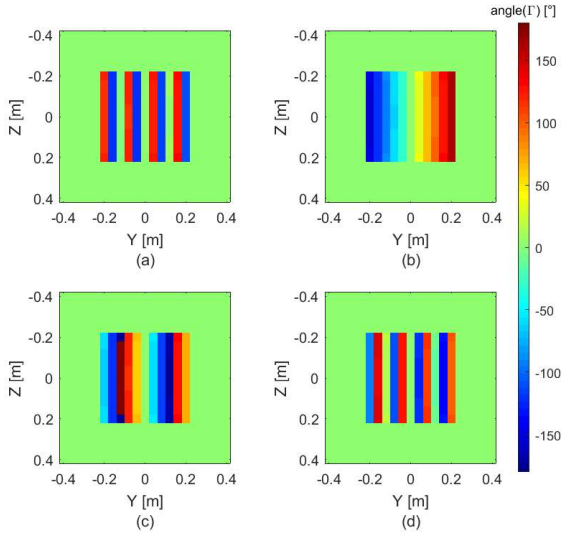

Figure 9. Required RIS phases in the 4 different cases for a wider beamwidth. (a) Case 1, (b) case 2, (c) case 3 and (d) case 4.

V. CONCLUSION

In this paper, a novel, fast and efficient method for codebook-based RIS configuration was proposed. The method involves using multiple level of beams with varying widths, which significantly reduces configuration overhead while maintaining the same performances as the conventional configuration method. It was also demonstrated that beams with multiple widths can be easily implemented using the same RIS.

REFERENCES

[1] V. Tapio, I. Hemadeh, A. Mourad, A. Shojaeifard, and M. Juntti, "Survey on Reconfigurable Intelligent Surfaces below 10 GHz", EURASIP Journal on Wireless Communications and Networking, 2021.

[2] E. Basar, "Present and Future of Reconfigurable Intelligent Surface-Empowered Communications", IEEE Future Networks 1st Massive MIMO Workshop, November 2021.

[3] M. M. Amri, N. M. Tran, and K. W. Choi, "Reconfigurable Intelligent Surface-Aided Wireless Communications: Adaptive Beamforming and Experimental Validations", IEEE Access, vol. 9, pp. 147442-147457, 2021.

[4] E. Björnson, H. Wymeersch, B. Matthiesen, P. Popovski, L. Sanguinetti, and E. de Carvalho, "Reconfigurable Intelligent Surfaces: A Signal Processing Perspective with Wireless Applications", in IEEE Signal Processing Magazine, vol. 39, no. 2, pp. 135-158, March 2022.

[5] C. Pan, H. Ren, K. Wang, J. F. Kolb, M. Elkashlan, M. Chen, M. Di Renzo, Y. Hao, J. Wang, A. L. Swindlehurst, X. You, and L. Hanzo, "Reconfigurable Intelligent Surfaces for 6G Systems: Principles, Applications, and Research Directions", in IEEE Communications Magazine, vol. 59, no. 6, pp. 14-20, June 2021.

[6] R. Liu, G. C. Alexandropoulos, Q. Wu, M. Jian, and Y. Liu, "How Can Reconfigurable Intelligent Surfaces Drive 5G-Advanced Wireless Networks: A Standardization Perspective", IEEE/CIC International Conference on Communications in China, Sanshui, Foshan, China, 2022, pp. 221-226, 2022.

[7] R. Liu, Q. Wu, M. Di Renzo, and Y. Yuan, "A Path to Smart Radio Environments: An Industrial Viewpoint on Reconfigurable Intelligent Surfaces", IEEE Wireless Communications, vol. 29, no. 1, pp. 202-208, February 2022.

[8] R. Liu, J. Dou, P. Li, J. Wu, and Y. Cui, "Simulation and Field Trial Results of Reconfigurable Intelligent Surfaces in 5G Networks", in IEEE Access, vol. 10, pp. 122786-122795, 2022.

[9] T. L. Jensen, and E. De Carvalho, "An Optimal Channel Estimation Scheme for Intelligent Reflecting Surfaces Based on a Minimum Variance Unbiased Estimator", IEEE International Conference on Acoustics, Speech and Signal Processing (ICASSP), pp. 5000-5004, Barcelona, Spain, 2020.

[10] X. Pei, H. Yin, L. Tan, L. Cao, Z. Li, K. Wang, K. Zhang, and E. Björnson, "RIS-Aided Wireless Communications: Prototyping, Adaptive Beamforming, and Indoor/Outdoor Field Trials", in IEEE Transactions on Communications, vol. 69, no. 12, pp. 8627-8640, December 2021.

[11] C. A. Balanis, "Antenna Theory Analysis and Design", 3rd edition, Wiley-Interscience, 2005.